Volume 10:1-12

UJEMI+

The Undergraduate Journal of Experimental Microbiology & Immunology (+Peer Reviewed)

Purified Ag43α Protein as a Potential Method for Preventing *Escherichia coli* Autoaggregation

Samantha Allum, Si An Chen, Sean Dang, Pranjali Singh

Department of Microbiology and Immunology, University of British Columbia, Vancouver, British Columbia, Canada

SUMMARY The phenomenon of *Escherichia coli* autoaggregation and the subsequent biofilm formation poses significant challenges in both healthcare and environmental spheres, primarily due to enhanced bacterial resistance against antibiotics. Autotransporters, particularly Antigen 43 (Ag43), a prominent outer membrane protein in Gram-negative bacteria like *E. coli*, facilitate bacterial aggregation through their distinct structural domains. Ag43 consists of a secreted passenger domain (Ag43α), an autochaperone domain and a β-barrel domain anchoring the secreted protein to the outer membrane. Previous studies have established the role of the Ag43α subunit in promoting aggregation through self-recognition. Hence, we hypothesise that the application of exogenously purified Ag43α could interrupt these intercellular interactions, thereby inhibiting autoaggregation. We expressed and purified the Ag43α subunit in BL21(DE3) strain of *E. coli* cells using the pEEKABOO plasmid from Leong et al. to investigate its influence on the aggregation of the Ag43-expressing DH5α *E. coli* strain. The results exhibited purified Ag43α protein adopting a stable tertiary structure post-translation. Furthermore, preliminary results from a single-trial aggregation assay revealed that introducing 200 μg/mL of purified Ag43α noticeably attenuated autoaggregation in acidic environments. Our preliminary findings provide a basis for further investigation of the Ag43α protein's potential in modulating *E. coli* autoaggregation and a possible avenue for the development of novel anti-biofilm therapeutics.

INTRODUCTION

Autotransporters (ATs) form the most substantial category of proteins secreted or situated in the outer membranes of Gram-negative bacteria. They are vital in aggregation and biofilm development which are essential for bacteria to withstand host immune responses and antibiotic treatments (1). Ag43 is a predominant protein found on the surface of some strains of *Escherichia coli*, classified within the AT family. It comprises several distinct domains: an N-terminal signal peptide, a secreted passenger domain known as Ag43α, an autochaperone domain aiding the folding process of the passenger domain, and a C-terminal β-barrel domain termed β43, which embeds itself into the outer membrane (2). Studies conducted by Klemm et al. suggest that the α-subunit, also referred to as the passenger domain, plays a pivotal role in the self-recognition and autoaggregation (bacterial clumping) behaviour exhibited by *E. coli* cells (3). This protein plays a crucial role in the autoaggregation and flocculation observed in static liquid cultures of *E. coli* across different strains, and it is also known to enhance the biofilm-forming capabilities of *E. coli* (4, 5).

Previous findings suggest the integral role of Ag43α in autoaggregation. Thus, we aim to explore the potential of utilising purified Ag43α protein to disrupt this process. Introducing purified Ag43α protein to a culture of *E. coli*, which expresses Ag43 on its cell surface, to

Published Online: September 2024

Citation: Allum, Chen, Dang, Singh. 2024. Purified Ag43α protein as a potential method for preventing *Escherichia coli* autoaggregation. UJEMI+ 10:1-12

Editor: Evelyn Sun, University of British Columbia

Address correspondence to:
https://jemi.microbiology.ubc.ca/

prevent autoaggregation stems from the understanding of Ag43α's self-interaction between *E. coli* cells (3). This protein is essential for autoaggregation and remains functional despite the deletion of two-thirds of the α-subunit (6). This suggests the potential of Ag43α in facilitating aggregation and reveals a possibility of leveraging Ag43α against itself to inhibit aggregation. It has been observed that the free form of the α-subunit of Ag43 is capable of reassociating with the β-subunit present in outer membrane extracts (7). This reveals that Ag43α has the potential to function as a complete protein independently of its attachment to the β-subunit. Hence, we hypothesised that the addition of purified Ag43α to *E. coli* cells, which exogenously express Ag43 on their surfaces, would suppress autoaggregation.

Additionally, the α-subunit can be isolated through heating at 60°C and purified through gel filtration and ion-exchange chromatography (7). However, for the purpose of our study, we chose to use the pET28a-Ag43passengerΔAC (pEEKABOO) plasmid in *E. coli* BL21(DE3) that uses the T7 expression system constructed by Leong et al. to obtain our Ag43α (8). The pEEKABOO plasmid encodes an N-terminally 6xHis-tagged Ag43 passenger protein without the autochaperone region (Ag43α) within a pET28a vector. The BL21(DE3) strain of *E. coli* contains the gene encoding the T7 RNA polymerase, while pET28a contains the T7 promoter along with a *lac* operator to suppress uninduced expression (9, 10). This allows for the expression of the encoded recombinant protein in the presence of isopropyl β-D-1-thiogalactopyranoside (IPTG). Furthermore, the 6xHis-tag at the N-terminal allows for the selection of our desired protein and hence its purification from other cellular components (11).

Therefore, to obtain purified Ag43α, we confirmed the expression of Ag43α protein in the *E. coli* BL21(DE3) pEEKABOO strain, purified the Ag43α protein, and demonstrated its solubility and retention of tertiary structure post-translation. Our preliminary but novel findings also display that the introduction of Ag43α reduces the aggregation rate of DH5α *E. coli* expressing Ag43 exogenously.

E. coli plays a crucial role in nosocomial infections due to its ability to acquire virulence factors through fimbrial adhesins, aggregation, and biofilm formation. Notably, studies utilising a murine model of UTI have demonstrated that Ag43a significantly enhances the long-term persistence of uropathogenic *E. coli* in the urinary bladder (12). Hence, this research not only deepens our understanding of *E. coli* autoaggregation but also opens new directions for developing therapeutic strategies aimed at preventing bacterial aggregation.

METHODS AND MATERIALS

Bacterial strains, plasmids, and cell cultures. All *E. coli* strains were obtained from the University of British Columbia (UBC). *E. coli* strains included BL21(DE3), BL21 containing pET28a, DH5α containing pBAD-Ag43 from AddGene, and BL21(DE3) containing pET28a-Ag43passengerΔAC (pEEKABOO) from Leong et al (8). Each strain was maintained on LB agar plates without antibiotics, with kanamycin (Kan) 50 μg/mL, with ampicillin (Amp) 100 μg/mL, and with Kan 50 μg/mL respectively. Antibiotic working concentrations for cultures grown in LB with Kan (LB+Kan) and LB with Amp (LB+Amp) are 50 μg/mL and 100 μg/mL respectively.

Transformation of pET28a in *E. coli* BL21(DE3) cells. *E. coli* BL21(DE3) containing pET28a was obtained to be used as an empty vector control by transforming pET28a plasmid into competent BL21(DE3) cells following protocols from Chang et al. (13). pET28a plasmid was extracted from BL21 pET28a using BioBasic EZ-10 Spin Column DNA Miniprep Kit (Cat: ST82316) following manufacturer protocols. Calcium chloride was used to make chemically competent BL21(DE3) cells following the protocols provided by Chang et al. (13).

Induction of Ag43α expression with IPTG. *E. coli* BL21(DE3) pET28a and BL21(DE3) pEEKABOO 5 mL LB+Kan cultures were grown overnight in the 37°C shaking incubator. Subcultures for each strain were prepared with 1 mL of overnight culture in 50 mL LB+Kan (50 μg/mL) and were grown in the 37°C shaking incubator until OD_{600} 0.4. All OD readings were measured using the Ultrospec 3000 UV/Visible Spectrophotometer (biochrom). 1 mL of each subculture was transferred to a microfuge tube for the uninduced control. 3 aliquots

were taken from each subculture and transferred to test tubes with IPTG stock solution for a final concentration of 0.5 mM IPTG and final volume of 2 mL. The test tubes were placed in the 37℃ shaking incubator for induction at 3 timepoints for each strain (1 hr, 2 hr, and 3 hr) to determine sufficient expression. For each strain, 150 µL of the uninduced and induced samples were aliquoted and spun down. The supernatant was removed and the pellets were stored at -20℃.

For Ag43α purification, protein expression was induced with IPTG for 1.5 hr. A BL21(DE3) pEEKABOO overnight culture was grown in 3 mL LB+Kan in the 37℃ shaking incubator. A subculture was prepared from 2 mL overnight culture in 100 mL LB+Kan and placed in the shaking incubator until OD_{600} 0.4. IPTG was added to 90 mL of subculture at a working concentration of 0.5 mM IPTG and placed in the shaking incubator for 1.5 hr. 80 mL of induced cells were pelleted and resuspended in 10 mL of sterile LB broth. Resuspended cells were transferred to 10 Eppendorf tubes in 1 mL aliquots which were pelleted. The supernatant was removed and the induced cell pellets were stored at -20℃.

Sodium dodecyl-sulphate polyacrylamide gel electrophoresis (SDS-PAGE). Cell or protein samples were diluted in 2x Laemlli buffer + 10% BME solution in a 1:1 ratio before boiling for 3-5 min at 95℃. Samples were further diluted if appeared not viscous. 10-15 µL of the sample was loaded onto SDS-PAGE gels prepared using the 10% TGX Stain-Free FastCast Acrylamide Kit (Bio-Rad, Cat: 165-0183) and ran in the BioBasic Mini-PROTEAN TetraCell as per manufacturer specifications (14). BioRad Precision Plus Protein Unstained Standards were used as a ladder. Gels were visualised on a BioRad GelDoc© system.

Cell lysis and isolation of Ag43α inclusion bodies. Cell pellets of *E. coli* BL21(DE3) BL21(DE3) pEEKABOO induced with IPTG for 2 hr and 3 hr were resuspended in 1X protease inhibitor cocktail solution (VWR, Cat: M221-1ML) diluted in dH_2O. Resuspended cells were then lysed with the MP FastPrep-24 homogenizer with 0.1 mm glass beads (BioSpec Products, Cat: 11079101) for 30 s at 6.0 m/s twice. Cell lysates were centrifuged at 15000 rpm for 1 min at 4°C to collect the soluble supernatant and insoluble pellets. The insoluble fraction was solubilized with solubilization buffer made with 10 mM Tris, 6 M urea, 2.5 mM imidazole, 0.5 M NaCl, 10 mM BME, and 20% glycerol, followed by 1 hr incubation on a shaker at room temperature. The suspension was centrifuged at 9500 rpm for 30 min, followed by loading the collected supernatant along with the soluble fraction on SDS-PAGE which was performed, as previously described, to identify the lysate fraction containing Ag43α inclusion bodies.

Ag43α purification using nickel resin immobilised metal affinity chromatography. Lysis and binding buffer, 5 mM imidazole wash buffer and 500 µM imidazole elution buffer were prepared according to the NEBExpress® Ni Resin Gravity Flow Typical Protocol under native conditions. Cell pellets were resuspended with 5 mL of lysis and binding buffer per gram of cells. Resuspended cells were lysed with the MP FastPrep-24 homogenizer with 0.1 mm glass beads (BioSpec Products, Cat: 11079101) with 20 s rounds at 6.0 m/s for 2 min total. Cell lysates were then centrifuged at 9600 rpm for 15 min to collect the soluble supernatant for subsequent protein purification performed at room temperature. 30 µL of the collected soluble fraction was aliquoted for downstream SDS-PAGE. 1 mL Ni resin (New England BioLabs, Cat: S1428S) was added into a 10 mL column and settled for 4 min, followed by equilibration using 5 mL lysis and binding buffer with the flowthrough being collected. 3.5 mL of the pooled supernatant samples were loaded into the column to interact with the resin for 10 min, allowing for protein binding. Resin was then washed with 10 mL 5 mM imidazole wash buffer to remove unbound or undesired bound proteins with flowthrough being collected. Ag43α bound to the resin was eluted and collected using 3 mL of 500 µM imidazole elution buffer. SDS-PAGE was performed, as previously described, using the soluble supernatant and collected flowthroughs to assess yield and purity of eluted Ag43α throughout the purification process.

Dialysis of purified Ag43α and protein quantification. Dialysis buffer was prepared with 20 mM Tris-HCl and 20 mM NaCl at pH 8.0 for a total of 3 L. Standard cellulose dialysis

tubing with 12000 to 14000 MWCO (Spectrum, Cat: S432706) was cut to 5 cm of length and soaked in 500 mL dialysis buffer. 1 mL purified Ag43α was loaded to the tubing and sealed tightly before stirring the tubing in dialysis buffer for 40 min and another time for 1 hr to wash off imidazole from the eluted protein sample. Dialysis buffer was replaced with fresh buffer after each wash. The last wash was done overnight at 4°C, followed by collection of imidazole-free Ag43α from the dialysis tubing. Dialysed protein samples were collected into 1.5 mL microfuge tubes. 2 µL aliquots were then loaded onto the NanoDrop 2000/2000c spectrophotometer (NanoDrop, Cat: ND2000CLAPTOP) to quantify the protein. Protein concentration was acquired for downstream assays using the molar extinction coefficient of 27960 M^{-1} cm^{-1} predicted by the ProtParam tool (https://web.expasy.org/protparam/) from Expasy (Swiss Bioinformatics Resource Portal) with the amino acid sequence of Ag43α. Samples were stored in -20°C until use.

Tertiary structure of Ag43α probed with limited proteolysis assay. Limited proteolysis protocol was adapted from Oliver et al. (15). Trypsin and trypsin inhibitors were prepared at 0.1 mg/mL, 0.01 mg/mL, and 0.001 mg/mL through serial dilution in 100 mM Tris pH 8.0 buffer on ice. BSA was prepared to 300 µg/mL in 20 mM Tris, 20 mM NaCl at pH 8.0 buffer. Purified Ag43α was kept at native concentration (265 µg/mL) in 20 mM Tris, 20 mM NaCl at pH 8.0 buffer. BSA and purified Ag43α were aliquoted into 25 µL samples before proteolytic induction. 1 µL from each trypsin dilution was added to each BSA and Ag43 aliquot prior to 15 min incubation at room temperature. Proteolytic reactions were then inhibited by adding 1 µL of trypsin inhibitor at a 1:1 mass ratio of trypsin protease to trypsin inhibitor. SDS-PAGE was performed by loading 12 µL aliquots from non-trypsinized BSA, trypsinized BSA, non-trypsinized non-dialyzed purified Ag43α, non-trypsinized Tris-dialyzed purified Ag43α, and trypsinized Tris-dialyzed purified Ag43α to assess Ag43α protein folding via proteolytic degradation outcomes and to initially probe the tertiary structure of Ag43α after protein expression. 10 µL of BioRad Precision Plus Protein Unstained Standards ladder was loaded to provide reference for band size.

Autoaggregation assay with addition of purified Ag43α. The aggregation assay was adapted from Klemm et al. (3). *E. coli* DH5α cells with pBAD-Ag43 were grown overnight at 37°C and 200 rpm in LB media supplemented with 100 µg/mL ampicillin. Overnight cultures were diluted 1:100 and grown to OD_{600} 0.4, at which point expression of Ag43 was induced by the addition of 0.2% arabinose, while control samples received 0.2% glucose and an equivalent volume of water. The cultures were grown for 75 min post-induction. Subsequently, 6 mL of cell culture per condition was harvested and resuspended in 5 mL of PBS with a pH value adjusted to 5. Two concentrations of purified Ag43 (20 µg/mL and 200 µg/mL) were then introduced into the PBS-suspended cell cultures. The cultures were maintained at room temperature throughout and were mixed vigorously for 15 s prior to the start of the assay. At 10-minute time intervals, a 100 µL sample was taken approximately 0.5 cm from the liquid surface and transferred onto a microtiter plate maintained on ice throughout the assay. The optical density was measured at 600 nm using the BioTek Epoch Microplate Spectrophotometer.

RESULTS

IPTG induces Ag43α expression in BL21(DE3) pEEKABOO. To confirm whether the *E. coli* strain BL21(DE3) containing pEEKABOO expresses Ag43α protein, we induced the cells with IPTG and performed SDS-PAGE. *E. coli* BL21(DE3) cells were induced with 0.5 mM IPTG at 3 timepoints (1 hr, 2 hr, and 3 hr) and whole cell lysate samples were run on a 10% SDS gel. Uninduced and empty vector controls using BL21(DE3) pET28a were included. Figure 1 shows the presence of a strong band at about 50 kDa (red arrow) in each of the test conditions lanes for the Bl21(DE3) pEEKABOO 1 hr, 2 hr, and 3 hr IPTG induction times. This band is not seen in the uninduced and empty vector control lanes. These results indicate that IPTG induction for 1 hr to 3 hr is sufficient for Ag43α protein expression in BL21(DE3) containing pEEKABOO.

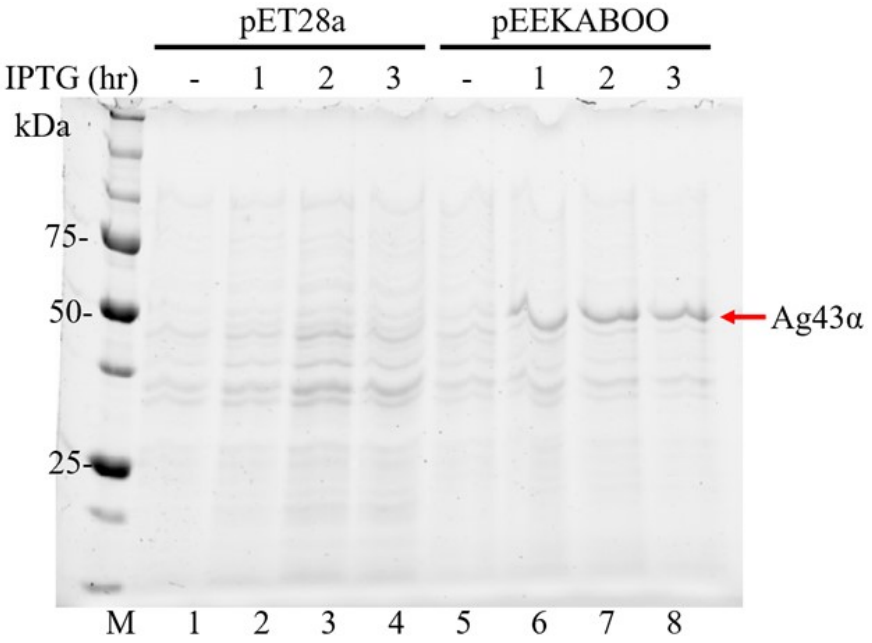

FIG. 1 Ag43α is expressed in BL21(DE3) containing pEEKABOO plasmid under IPTG induction. SDS-PAGE gel loaded with whole cell lysate samples of BL21(DE3) cells containing pET28a or pEEKABOO plasmid, uninduced or induced with 0.5 mM IPTG for 1 hr, 2 hr, or 3 hr. The ladder used was BioRad Precision Plus Protein Unstained Standards, indicated as Lane M.

Ag43α eluted from the Ni column is relatively pure and concentrated. After confirming protein expression from pEEKABOO, nickel affinity chromatography was used to perform Ag43α purification (Fig. 2). The soluble protein fraction was collected upon centrifugation of cell lysates with some reserved for downstream SDS-PAGE. The rest of the supernatant was loaded into a column with equilibrated nickel resin for protein binding. Off-target protein contamination was washed away, followed by elution of his-tagged Ag43α. Flowthroughs from the binding, washing, and elution steps were also collected for SDS-PAGE to assess the yield and purity of Ag43α throughout the purification process (Fig. 2).

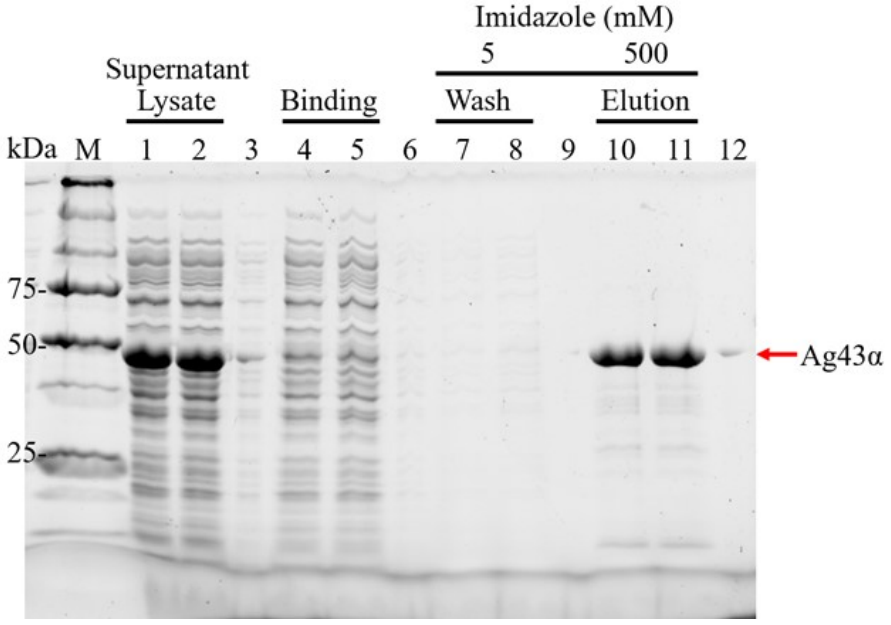

FIG. 2 Ag43α was purified with nickel affinity chromatography. Soluble protein fraction from IPTG-induced pEEKABOO-transformed BL21(DE3) cells was purified with nickel affinity chromatography. SDS-PAGE was loaded with aliquots from the soluble supernatant obtained prior to purification and flowthroughs of the binding, wash, and elution steps throughout purification. The lane labelled M holds the unstained protein ladder.

The gel image displays multiple bands across the lanes loaded with the soluble fraction with particular strong bands around 50 kDA. This indicates a relatively low purity and high amounts of Ag43α in the protein sample prior to the purification process as expected. For lanes loaded with the binding and washing flowthroughs, a similar amount of bands was observed but with a lower intensity, indicating the removal of unbound and undesired protein molecules. The eluted protein samples resulted in strong bands around 50 kDA and some undesired weaker bands at lower molecular weights. Therefore, the overall band patterns in the gel suggest Ag43α eluted from the nickel column being relatively pure and concentrated.

Purified Ag43α is Folded in its Tertiary Structure. To confirm the tertiary structure of Ag43α after expression and purification, we performed limited proteolysis on purified Ag43α with various concentrations of trypsin (Fig. 3). Specifically, 25 µL aliquots of Ag43α at native concentrations (265 µg/mL) were treated with 0.1 mg/mL, 0.01 mg/mL, and 0.001 mg/mL of trypsin for 15 min. Upon treatment completion, the trypsinized samples were run on a 10% SDS gel. Trypsinized and non-trypsinized 300 µg/mL BSA, non-trypsinized Ag43α, and non-trypsinized non-dialyzed Ag43α were used as controls. In the gel image, each BSA lane shows a visible band between 50 and 75 kDa. We also observe strong bands at 50 kDa for the Ag43α controls and 0.001 mg/mL trypsinized Ag43α. For each of the trypsinized Ag43α samples, fainter cascading bands follow below the 50 kDa point, increasing in intensity with each increase in trypsin concentration. These results indicate Ag43α tertiary structure-mediated protection against proteolysis.

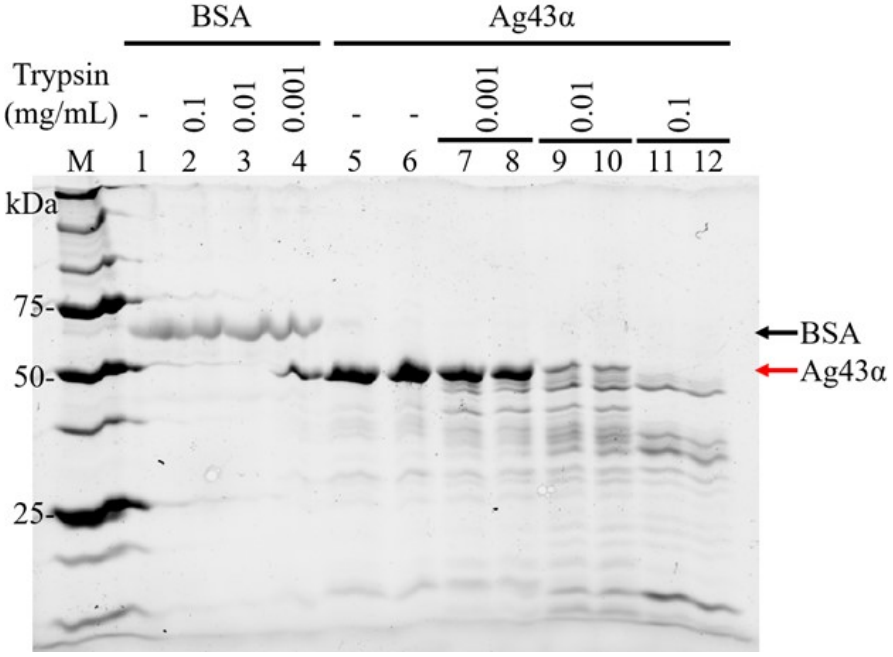

FIG. 3 Purified Ag43α is folded with a tertiary structure. SDS-PAGE was loaded with samples of either 300 µg/mL BSA and 265 µg/mL Ag43α. Lanes labelled 1 to 4 held BSA samples with no trypsin treatment and 0.1, 0.01, and 0.001 mg/mL trypsin treatment respectively. Lane 5 was loaded with non-dialyzed Ag43α with no trypsin treatment. Lanes 6 to 12 held Tris-dialyzed Ag43α samples with paired treatments of no trypsin and 0.1, 0.01, and 0.001 mg/mL trypsin respectively. The lane labelled M holds the unstained protein ladder.

Reduced aggregation observed with the addition of Ag43α to aggregating DH5α expressing pBAD-Ag43. To investigate the impact of purified Ag43α on the autoaggregation of DH5α *E. coli* expressing pBAD-Ag43, an aggregation assay using varying concentrations of our purified Ag43α, which was expressed from the pEEKABOO plasmid. The experimental procedure entailed growing *E. coli* DH5α containing pBAD-Ag43 to an OD_{600} of 0.4, inducing Ag43 expression with 0.2% arabinose, and resuspending the cultures in pH 5 PBS with subsequent addition of 20 µg/mL or 200 µg/mL purified Ag43α. Controls included water and induction with 0.2% glucose as it represses the pBAD expression system. A reduced aggregation rate was observed in the presence of 200 µg/mL Ag43α, and a less dramatic reduction occurred with 20 µg/mL Ag43α (Fig. 4A). Furthermore, a notable OD_{600} difference of about 0.4 to 0.55 is observed over 20 min of the aggregation assay between the arabinose-induced control and the culture with 200 µg/mL Ag43α protein added (Fig. 4B). These findings suggest that Ag43α plays a role in impeding autoaggregation of DH5α *E. coli* expressing Ag43 in an acidic environment.

DISCUSSION

In this study, we induce and purify Ag43α protein from an *E. coli* protein expression system. Probing of the tertiary structure reveals that Ag43α remains folded following purification. Preliminary findings from autoaggregation assay tests indicate the addition of the purified protein to *E. coli* expressing Ag43 could inhibit autoaggregation under acidic conditions.

Induction and protein expression. The pEEKABOO plasmid in BL21(DE3) was obtained from Leong et al. (Supplementary Figure S1) (8). To obtain purified Ag43α for downstream analysis, we aimed to confirm that Ag43α is expressed under IPTG induction.

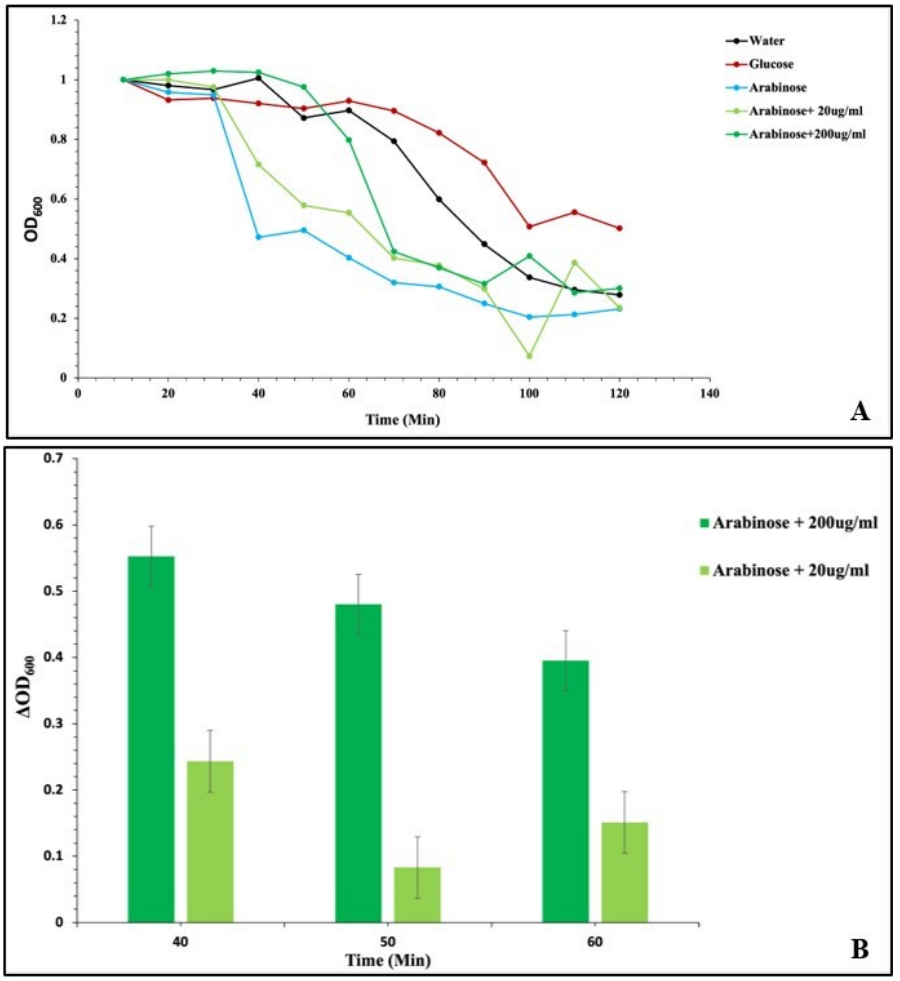

FIG. 4 Reduced aggregation with the addition of Ag43α protein to the aggregation assay of DH5α expressing pBAD-Ag43. (A) Ag43 induction with 0.2% glucose and arabinose initiated upon overnight subculture reaching an OD_{600} of 0.4, followed by a 75-min incubation. Post-incubation, cultures were resuspended in PBS, with aggregation rates assessed via OD_{600} readings, normalised and recorded at 10-min intervals over a 2 hr period. (B) Graphical representation of normalised OD differentials at peak time points, comparing arabinose-induced control with additions of 20 µg/mL and 200 µg/mL Ag43α protein.

IPTG prevents the repressor from binding the *lac* operon which allows T7 RNA polymerase to bind the T7 promoter, resulting in protein expression (9). To determine the optimal time for protein expression, different induction times were tested. The resulting SDS gel had a band in the pEEKABOO lanes for each IPTG induction time which matched the predicted molecular weight of Ag43α of about 50 kDa (Figure 1). This band was not present in the uninduced and empty vector control lanes. Therefore, induction with 0.5 mM IPTG for 1 to 3 hr results in Ag43α protein expression in the BL21(DE3) pEEKABOO cells. The Ag43α band appeared to be relatively similar in strength between the 3 time points. Thus, IPTG induction for 1 to 3 hr is sufficient for protein expression. However, different conditions for induction can be investigated to increase protein yield.

Protein purification. After IPTG induction experiments, the cell lysate protein fraction containing Ag43α inclusion bodies was identified by SDS-PAGE to decide the appropriate protocol for protein purification (Supplementary Figure S2). The resulting gel image shows numerous bands in the soluble protein fraction with a stronger signal at around 50 kDa for induced samples, indicating the presence of Ag43α inclusion bodies. Intriguingly, this was not observed for the insoluble protein fraction as high expression of recombinant protein typically leads to insoluble inclusion bodies (16). This implies that Ag43α possesses an amino acid sequence and protein structure with properties such as net charge, hydrophilicity, and size that promote proper folding and solubility in the cytoplasmic environment (17). This is further implied in our downstream limited proteolysis assay (Fig. 3). Further investigation would be required to elucidate the solubilizing characteristics of Ag43α. Nonetheless, we proceeded with a purification protocol tailored for proteins under native conditions, removing the need to include a refolding step in our experimental workflow.

Immobilised metal affinity chromatography involves the electrostatic attractions between the 6xHis tag of recombinant proteins and transition metal ions such as nickel (Ni^{2+}) that are immobilised on resin matrices in columns (11). After the application of the soluble fraction

into the column for protein binding, a buffer with low levels of imidazole is typically used to wash away proteins that are weakly or non-specifically bound to the resin (11). This is then followed by eluting the his-tagged proteins with high concentrations of imidazole (11). The resulting gel image from loading the collected flowthroughs throughout the purification process in SDS-PAGE shows band patterns that indicate relatively pure and concentrated Ag43α upon elution (Fig 2.). However, non-target proteins were observed alongside Ag43α in our eluted sample in the form of lower molecular weight bands (Fig. 2). These lower bands in the elution lanes possibly correspond to smaller proteins with histidine residues or clusters weakly bound to the nickel resin that were not entirely removed with the 5 mM imidazole wash buffer. Another possibility would be truncated or cleaved Ag43α with the 6xHis tag as a result of unwanted proteolysis. During the cell lysis procedure, we did not include any protease inhibitor to the lysis buffer used to resuspend the cell pellets as it was not explicitly mentioned in the manufacturer's protocol. Uninhibited proteases would result in Ag43α protein fragments strongly bound to the resin due to the 6xHis tag which can only be removed with high levels of imidazole during the elution step. Future studies could further optimise the purification process to obtain Ag43α at higher purity while maintaining a sufficient yield for downstream analysis.

Limited proteolysis. After determining the solubility of purified Ag43α, limited proteolysis was performed to confirm the tertiary folding of the protein after expression and purification. Limited proteolysis uses the concept that a protein folded in its tertiary structure will be better protected against protease digestion (18). In theory, fewer lysine (Lys) and arginine (Arg) residues will be exposed in proteins in tertiary conformation, as trypsin selectively cleaves C-terminal lysine and arginine residues (19). We hypothesised that if Ag43α is linear, there would be a complete absence of bands, as trypsin would have complete access to every Lys and Arg residue, cleaving the protein into untraceable strands. The limited proteolysis results were assessed using SDS-PAGE, where we observe strong bands at 50 kDa in the 0.001 mg/mL trypsin-treated Ag43α samples. The presence of these 50 kDa bands suggests that Ag43α, which is 50 kDa in length, is folded in its tertiary structure, conferring protection against trypsin digestion. While the band at 50 kDa becomes fainter for the 0.01 and 0.1 mg/mL trypsin-treated Ag43α samples, the cascading bands below this point suggest that these higher concentrations of trypsin begin to probe the structure of Ag43α (20). This is further supported by the presence of relatively stronger bands at certain sizes, revealing particular points of Lys or Arg exposure in the tertiary structure of Ag43α (19). Interestingly, these results suggest that Ag43α may be able to fold into its tertiary structure without the aid of its autochaperone domain (21), whereas the Type V transporter BrkA, a similar protein, does (14). This necessitates further research on the involvement of the autochaperone domain and other chaperone proteins in Ag43 folding.

As positive controls, non-trypsinized Ag43α that were Tris-dialyzed and non-dialyzed were included in analysis. Again, a strong band at 50 kDa was observed for each of these samples, providing the size of Ag43α before trypsinization (8). As a proof of concept, BSA was used to confirm that a folded protein indeed protects against limited proteolysis. As hypothesised, we observed visible bands for each trypsin treatment concentration of BSA at a single point between 50 and 75 kDa. This is confirmed by the size of BSA, being 66 kDa or 585 amino acids in length (22). These findings validate the protocols of IPTG induction for Ag43α expression and Ni-column affinity chromatography for Ag43α purification.

Aggregation assay. The role of Ag43 in the autoaggregation of *E. coli* cells has led to notable insights within our current study. Based on prior research indicating the role of Ag43α in autoaggregation, our investigation aimed to discern the effects of purified Ag43α on this process (3). Despite the deletion of substantial portions of the alpha subunit, *E. coli* cells continued to aggregate, hinting at the influence of Ag43α in mediating this process (6). We added purified Ag43α to an *E. coli* culture with exogenous Ag43 expression, postulating that such addition could decrease autoaggregation through the protein's self-interacting properties (7, 8).

Preliminary experiments using the fimbriae-positive DH5α *E. coli* strain containing pBAD-Ag43 revealed the absence of aggregation patterns in standard ampicillin-treated LB media. Previous studies reveal that fimbriation can block Ag43-mediated autoaggregation of *E. coli* and that acidic conditions downregulate fimbriae expression (23, 24). An aggregation

assay confirmed the expected autoaggregation at pH 5 in the presence of arabinose (Supplementary Figure S3). Therefore, all further aggregation tests were performed under acidic conditions.

In our initial experiment, we observed a noticeable reduction in the autoaggregation of 0.2% arabinose-induced *E. coli* DH5α, exogenously expressing Ag43, upon the addition of our purified Ag43α protein. The addition of 200 µg/mL Ag43α demonstrated a reduced aggregation rate compared to the 0.2% arabinose-induced control, while 20 µg/mL Ag43α displayed comparatively smaller reduction in aggregation (Fig 4A). Figure 4B highlights the OD_{600} difference observed between the arabinose-induced control and the cultures with 200 µg/mL and 20 µg/mL Ag43α added. Additionally, increased clumping of cells settling at the bottom of the culture tube was observed in aggregating samples. Hence, these preliminary findings support our hypothesis by showcasing the possible role of Ag43α in exerting an inhibitory effect on autoaggregation in an acidic environment. This is supported by previous findings that Ag43α can self-interact and self-recognize (1). Hence, it is plausible that purified and folded Ag43α attaches to Ag43 expressed on the surface of *E. coli* DH5α, interrupting the self-recognition between Ag43.

To further explore our preliminary findings, a supplementary follow-up experiment involving BSA as a control was conducted. However, this experiment was inconclusive due to experimental design and time constraints. Nevertheless, we highlight the importance of several notable factors to consider for future experiments. The data from this experiment suggests that our water control is indicative of a possible leaky expression of Ag43. The addition of 20 µg/mL Ag43α displayed similar aggregation patterns to the arabinose control, contrasting our preliminary findings (Supplementary Figure S4). However, the addition of 200 µg/mL Ag43α resulted in relatively reduced but visible prevention of aggregation, which follows the trend that increasing concentrations of Ag43α inhibits autoaggregation more effectively. Although the addition of BSA also showed an aggregation-reducing effect, it was less effective than 200 µg/mL Ag43α, highlighting the specificity of Ag43α in moderating the autoaggregation phenomenon.

It is important to consider the experimental modifications that occurred during this assay, which involved a change in protocol from the initial assay. These alterations included differences in the volume of PBS used for resuspension and the used spectrophotometer. In addition, changes in the volume measured for optical density, particularly at the 30-minute mark where a lower than intended volume was used, resulted in an inconsistent data point. The initial primary assay was run for 20 min, with the removal of about 1 mL of culture for OD readings. We then restarted the assay by briefly vortexing all the cultures before taking OD readings The potential alteration of protein concentration due to the removal of culture for initial assay measurements and the unknown binding affinity of Ag43α interactions, which may not have been affected by vortexing, call for cautious interpretation of this experiment. Despite these limitations, the consistency observed in the reduction of autoaggregation with the addition of 200 µg/mL Ag43α supports our conclusion that Ag43α has a role in moderating autoaggregation in *E. coli* DH5α under the tested experimental conditions. Additionally, Supplementary Figure 4 showcases the importance of considering factors involved in the dynamics of Ag43-facilitated autoaggregation, such as cell concentration, Ag43α concentration, and measurement time.

Our data provides preliminary evidence that Ag43α plays a role in attenuating the aggregation of DH5α *E. coli* cells expressing Ag43. However, future studies are needed to validate our experimental findings and extend the understanding of Ag43α's binding properties and interactions to fully elucidate its inhibitory mechanism of action. These insights provide a stepping stone to further inquire into the applications of Ag43α, with an emphasis on understanding its interaction dynamics and exploring its full therapeutic potential against bacterial aggregation and biofilm formation.

Limitations In future studies, regarding limited proteolysis, it would be optimal to include a protein with a confirmed linear structure, such as the unfolded BrkA passenger domain lacking a Glu^{601}–Ala^{692} junction (15), to provide a reference for how linear proteins would appear on the SDS-PAGE gel after limited proteolysis.

For aggregation kinetics, Vo et al. have explored the specific interactions between amino acids at the contact interfaces of adjacent Ag43 proteins, which facilitate a common mode of trans-association leading to cell aggregation (23). Furthermore, they describe how slight variations in these interactions can alter the kinetics of aggregation and the compactness of cell clusters (23). This aspect of Ag43α's binding affinity and molecular interaction was not considered in our study. We also acknowledge the feasibility limits for our aggregation assay, which include the potential changes in the solubility and structure of Ag43α at pH 5 as well as the possibility of Ag43α binding to itself rather than to the wild-type Ag43 on the *E. coli* cell surface. These factors could have a substantial impact on the dynamics of aggregation and represent areas for future investigation.

Conclusions The findings obtained provide insight into the role of Ag43α in autoaggregation in *E. coli*. Through the transformation of the pET28a plasmid, we provide a working protocol for Ag43α expression and purification. Furthermore, through solubility analysis and limited proteolysis, we have confirmed the soluble nature and tertiary structure of Ag43α post-expression. This study also provides an optimised autoaggregation assay protocol to assess the dynamics between purified Ag43α and autoaggregation in *E. coli*. The result of the autoaggregation assay suggests that purified Ag43α can be used as a potential method to disrupt or inhibit autoaggregation. Taken together, these working protocols and preliminary findings offer a direction towards exploring the mechanisms of *E. coli* aggregation and provide an avenue for developing novel therapeutics for bacterial biofilm formation.

Future Directions Future studies may further optimise the induction and purification process to obtain Ag43α at higher yield and purity. This study tested different IPTG induction times; however, other variables can be adjusted for higher yield. This includes adjusting the concentration of IPTG, the temperature at induction, or optimising the induction medium (25). One should consider slightly increasing the imidazole concentration of the wash buffer to remove histidine-containing contamination more effectively, albeit with the cost of Ag43α yield.

Furthermore, studies could test various reagents, concentrations, and pH for an optimal dialysis buffer to remove imidazole from the eluted Ag43α. In this study, the dialyzed protein remained stable in Tris buffer (20 mM Tris-HCl and 20 mM NaCl at pH 8.0) and was used for experiments. However, another dialysis was performed with a phosphate buffer (20 mM sodium phosphate and 300 mM NaCl at pH 7.4) which resulted in protein precipitation. Alternative buffers may be investigated to lower the risk of protein aggregation and keep Ag43α stable for experimental use or storage.

The autoaggregation assay should be repeated while including technical replicates and standard protein as protein vector controls to support our preliminary findings. Additionally, to better understand the limits of Ag43α function in the presence of other conditions, further optimised aggregation assays under different pH, NaCl, knockouts of *fimA, fimB*, and *fimH*, and osmolarity conditions can be done. Moreover, to confirm that cells are attenuated for autoaggregation, DIC/phase contrast imaging and images of the aggregated cell clumps in the bottom of the culture tubes should be considered. Further studies can also include a biofilm assay to assess the effect of purified Ag43α on the biofilm-forming capabilities of *E coli*. This would open up possible avenues in the development of therapeutics against biofilm formation.

Lastly, all aforementioned experiments should be repeated with a pEEKABOO plasmid containing a functional autochaperone region set up as a control. However, this would likely involve extensive optimization of parameters in induction, inclusion bodies isolation, purification, dialysis, and downstream assays.

ACKNOWLEDGEMENTS

We would like to extend our sincere gratitude to the MICB 471 teaching team, with special thanks to David Oliver and Shruti Sandilya for their invaluable guidance, expertise, and encouragement throughout the development of our project. We are also grateful to Jade Muileboom for her mentorship and support in the laboratory, which has been instrumental in helping us achieve our research objectives. Furthermore, we appreciate our peers for their

collaborative spirit, which has memorably contributed to the success of our endeavours. Additionally, we would like to acknowledge the Microbiology and Immunology Department at the University of British Columbia Vancouver for their financial support and the provision of resources that have been crucial in reaching our project goals. We would also like to thank the anonymous reviewers for constructive feedback on this manuscript.

CONTRIBUTIONS

All authors collaborated to prepare this manuscript. S.K.A. contributed to the title, introduction, methods, figures, results, discussion, future directions, references, and supplementary material. S.A.C. contributed to the methods, results, discussion, future directions, references, and supplementary material. S.D. contributed to the methods, results, discussion, and conclusion. P.S. contributed to the title, abstract, introduction, methods, figures, results, discussion, limitations, acknowledgements, and supplementary material.

REFERENCES

1. **Heras B, Totsika M, Peters KM, Paxman JJ, Gee CL, Jarrott RJ, Perugini MA, Whitten AE, Schembri MA.** 2014. The antigen 43 structure reveals a molecular Velcro-like mechanism of autotransporter-mediated bacterial clumping. *Proc Natl Acad Sci U S A* **111**:457–462.
2. **van der Woude MW, Henderson IR.** 2008. Regulation and function of Ag43 (flu). *Annu Rev Microbiol* **62**:153–169.
3. **Klemm P, Hjerrild L, Gjermansen M, Schembri MA.** 2004. Structure-function analysis of the self-recognizing Antigen 43 autotransporter protein from *Escherichia coli*. *Mol Microbiol* **51**:283–296.
4. **Diderichsen B.** 1980. flu, a metastable gene controlling surface properties of *Escherichia coli*. *J Bacteriol* **141**:858–867.
5. **Kjaergaard K, Schembri MA, Ramos C, Molin S, Klemm P.** 2000. Antigen 43 facilitates formation of multispecies biofilms. *Environ Microbiol* **2**:695–702.
6. **Najera Mazariegos A, McDonald K, Tepes M, Zhang S.** Morphological and functional characterization of the C-terminal two-thirds of the autotransporter Ag43 alpha domain via site-directed mutagenesis in *Escherichia coli* DH5α. Submitted for publication in *Undergrad J Exp Microbiol Immunol* January 2023.
7. **Caffrey P, Owen P.** 1989. Purification and N-terminal sequence of the alpha subunit of antigen 43, a unique protein complex associated with the outer membrane of *Escherichia coli*. *J Bacteriol* **171**:3634–3640.
8. **Leong R, Safaeian S, Zhang J.** Construction of a plasmid that expresses an N-terminally 6xHis tagged protein spanning amino acids Gly139 to Pro552 of the passenger domain of the *Escherichia coli* autotransporter protein Ag43. Submitted for publication in *Undergrad J Exp Microbiol Immunol* January 2023.
9. **Du F, Liu Y-Q, Xu Y-S, Li Z-J, Wang Y-Z, Zhang Z-X, Sun X-M.** 2021. Regulating the T7 RNA polymerase expression in *E. coli* BL21 (DE3) to provide more host options for recombinant protein production. *Microb Cell Factories* **20**:189.
10. **Shilling PJ, Mirzadeh K, Cumming AJ, Widesheim M, Köck Z, Daley DO.** 2020. Improved designs for pET expression plasmids increase protein production yield in *Escherichia coli*. *Commun Biol* **3**:214.
11. **Kanoh S, Shiraki K, Wada M, Tanaka T, Kitamura M, Kato K, Hirano A.** 2023. Chromatographic purification of histidine-tagged proteins using zirconia particles modified with phosphate groups. *J Chromatogr A* **1703**:464112.
12. **Ulett GC, Valle J, Beloin C, Sherlock O, Jean-Marc Ghigo, Schembri MA.** 2007. Functional Analysis of Antigen 43 in Uropathogenic *Escherichia coli* Reveals a Role in Long-Term Persistence in the Urinary Tract. *Infection and Immunity* **75**:3233–3244.
13. **Chang AY, Chau VW, Landas JA, Pang Y.** 2017. Preparation of calcium competent *Escherichia coli* and heat-shock transformation. *Undergrad J Exp Microbiol Immunol* **1**:22–25.
14. **BioRad.** TGX™ and TGX Stain-Free™ FastCast™ Acrylamide Kit and Starter Kit Instruction Manual. BioRad.
15. **Oliver DC, Huang G, Nodel E, Pleasance S, Fernandez RC.** 2003. A conserved region within the *Bordetella pertussis* autotransporter BrkA is necessary for folding of its passenger domain. *Mol Microbiol* **47**:1367–1383.
16. **Singh A, Upadhyay V, Upadhyay AK, Singh SM, Panda AK.** 2015. Protein recovery from inclusion bodies of *Escherichia coli* using mild solubilization process. *Microb Cell Factories* **14**:41.
17. **Wilkinson DL, Harrison RG.** 1991. Predicting the Solubility of Recombinant Proteins in *Escherichia coli*. *Nat Biotechnol* **9**:443–448.
18. **Carey J.** 2000. A systematic and general proteolytic method for defining structural and functional domains of proteins. *Methods Enzymol* **328**:499–514.
19. **Olsen JV, Ong S-E, Mann M.** 2004. Trypsin cleaves exclusively C-terminal to arginine and lysine residues. *Mol Cell Proteomics MCP* **3**:608–614.

20. **Zappacosta F, Pessi A, Bianchi E, Venturini S, Sollazzo M, Tramontano A, Marino G, Pucci P.** 1996. Probing the tertiary structure of proteins by limited proteolysis and mass spectrometry: the case of Minibody. *Protein Sci* **5**:802–813.
21. **Jing K, Guo Y, Ng I-S.** 2019. Antigen-43-mediated surface display revealed in *Escherichia coli* by different fusion sites and proteins. *Bioresour Bioprocess* **6**:14.
22. **Carter DC, Ho JX.** 1994. Structure of Serum Albumin. *Adv Protein Chem* **45**:153-203.
23. **Vo JL, Ortiz GCM, Totsika M, Lo AW, Hancock SJ, Whitten AE, Hor L, Peters KM, Ageorges V, Caccia N, Desvaux M, Schembri MA, Paxman JJ, Heras B.** 2022. Variation of Antigen 43 self-association modulates bacterial compacting within aggregates and biofilms. *Npj Biofilms Microbiomes* **8**:20.
24. **Hasman H, Chakraborty T, Klemm P.** 1999. Antigen-43-Mediated Autoaggregation of *Escherichia coli* Is Blocked by Fimbriation. *J Bacteriol* **181**:4834–4841.
25. **Sivashanmugam A, Murray V, Cui C, Zhang Y, Wang J, Li Q.** 2009. Practical protocols for production of very high yields of recombinant proteins using *Escherichia coli*. *Protein Sci* **18**:936–948.